

Convective instabilities of a normal liquid ^3He - ^4He mixture

H. Gao and R. P. Behringer

Department of Physics, Duke University, Durham, North Carolina 27706

(Received 23 September 1985)

We report studies of Nusselt number N versus Rayleigh number R for a normal liquid ^3He - ^4He mixture with ^3He mass concentration $c = 0.038$, confined in cylindrical containers with aspect ratios, Γ (radius/height) of $5.5 \leq \Gamma \leq 10.2$. These data were obtained for separation ratios ψ of $-0.2 \lesssim \psi \lesssim 0.1$. For $\psi > 0$, the data are consistent with predictions that the slope RdN/dR is small just above the onset of convection and then increases with R . For $\psi = 0$, N is a concave function of R with $N \propto (R - R_{cs})^{1/2}$. Contrary to predictions for a horizontally infinite layer, no oscillations at onset were found for $\psi < 0$. Above the onset of convection when $\psi < 0$, we observed additional transitions which are beyond the scope of current theory.

Rayleigh-Benard convection in a pure fluid has received considerable attention because it provides a useful system for testing theories of nonlinear dynamics.^{1,2} Recently, there has been interest in the corresponding problem in a binary mixture.³⁻¹⁰ A number of phenomena which do not apply to a pure fluid are predicted⁶⁻⁹ to occur in a binary mixture; these phenomena include an analog to a thermodynamic tricritical point and a codimension-two bifurcation. Both mixtures in a porous medium and unconfined or bulk mixtures are predicted to show these features. Here, we report a test of these predictions by means of heat-transport measurements on bulk convecting layers. The fluid was a normal ^3He - ^4He mixture with a ^3He mass concentration of $c = 0.038$. Although we find some qualitative agreement with theory, there remain important differences between our measurements and recent predictions.⁶ In addition, we have found a set of transitions occurring after the onset of convection which are beyond the scope of recent theory.

In the normal phase, where the temperature T is greater than the superfluid temperature $T_\lambda(c)$, a ^3He - ^4He mixture is a Newtonian fluid. During the present experiments, a normal mixture layer was confined by cylindrical sidewalls in an apparatus¹¹ which allowed us to vary *in situ* the aspect ratio $\Gamma = \delta/2d$, with δ the diameter and d the height of the layer. Several other parameters describe the flow state,⁶ among them the Rayleigh number $R = \beta_1 g d^3 \Delta T / \kappa \nu$, the separation ratio $\psi = -k_T \beta_2 / T \beta_1$, the Lewis number $L = D/\kappa$, and the Prandtl number $P = \nu/\kappa$. These quantities are formed from $\beta_1 = -\rho^{-1}(\partial\rho/\partial T)_{P,c}$; $\beta_2 = -\rho^{-1}(\partial\rho/\partial c)_{P,T}$; ν , the kinematic viscosity; κ , the thermal diffusivity; D , the mass diffusion coefficient; and k_T , the thermal diffusion ratio.¹² Here, g is the acceleration of gravity, and ΔT is the temperature difference across the layer. We present our heat-transport measurements in the form of a Nusselt number, N . N is defined as the actual heat-flux Q carried by the layer normalized by the heat flux needed to sustain the same R in the absence of convection.

The Lewis and Prandtl numbers vary relatively slowly with T and c , except near T_λ .¹² In these experiments $P = 0.63$, and L varies between 3×10^{-2} and 5×10^{-2} . The quantities contained in ψ vary significantly and have high

uncertainties near T_λ .¹³ Near $T_\lambda + 0.1$ K we expect that $k_T = \psi = 0$. For temperatures higher than this, $\psi > 0$; for lower temperatures $\psi < 0$, and ψ approaches $-\infty$ for T approaching $T_\lambda + 0.01$ K from above. In the present work, the mean temperature is varied near the point where ψ is expected to be zero, and the experiments included the range $-0.2 \lesssim \psi \lesssim 0.1$.

When a mixture layer is heated from below, as in the present experiments, several phenomena are predicted⁶⁻⁹ to occur near the onset of convection, depending on the value of ψ . If the equations of motion are linearized about the purely conductive state, two types of instabilities may occur: one to a steady convective state with a critical Rayleigh number R_{cs} , and the other to an oscillatory convective state with a critical Rayleigh number R_{co} . $R_{co} < R_{cs}$ when $\psi < \psi_{pc} < 0$; the reverse is true when $\psi > \psi_{pc}$. The two curves $R_{cs}(\psi)$ and $R_{co}(\psi)$ intersect at ψ_{pc} , the polycritical value of ψ . This intersection yields a codimension-two bifurcation point,^{6,14} and a number of interesting phenomena are predicted to occur in its vicinity. The bifurcation to stationary convection is predicted to change from a forward to a backward bifurcation at ψ_t , with $\psi_{pc} < \psi_t < 0$, and at ψ_t a hydrodynamic analog of a tricritical point^{6,7} is to occur.

We note that many theoretical predictions, in particular those regarding the tricritical point and codimension-two phenomena, have been obtained using boundary conditions (such as slip boundaries) at the horizontal surfaces which simplify calculations, but do not rigorously apply to experiments.¹⁵ The effects of using unphysical boundary conditions are not easily determined, in general, but an indication can be obtained by comparing values of R_{cs} obtained using rigid boundary conditions versus the slip conditions often imposed in the calculations. For example, when $\psi = 0$, rigid boundary conditions applied to a horizontally infinite bulk layer yield $R_{cs} = 1708$, whereas the slip conditions yield $R_{cs} = 658$. These two results differ by a factor of 2.6.

Although calculations using slip boundary conditions are not quantitatively applicable to experiments, they provide a framework for discussing laboratory results. One such calculation by Brand, Hohenberg, and Steinberg⁶ (BHS) which is useful here is that for bulk mixtures

$\psi_t = -L^3/(1+L+L^2+L^3)$. For $L=0.04$, as in our experiments, ψ_t for this prediction is quite close to zero: $\psi_t = -6 \times 10^{-5}$. BHS⁶ also predict ψ_{pc} for slip boundary conditions:¹⁵ $\psi_{pc} = -L^2(1+P)/[L^2+L)(1+P)+P]$. For $L=0.04$ and $P=0.63$, this yields $\psi_{pc} = -3.7 \times 10^{-3}$. Again using slip boundary conditions, BHS⁶ predict that just above the onset of steady convection N should vary to lowest order in $\varepsilon_s = (R - R_{cs})/R_{cs}$, as $N = 1 + N_{1s}\varepsilon_s$, with

$$N_{1s} = 2(1 - \psi/\psi_t - \psi L^{-3})/(1 - \psi/\psi_t). \quad (1)$$

This result is to hold, provided that the stationary instability leads to a forward bifurcation. Equation (1) is the result of a relation for the convective amplitude¹⁶ B : $B = \varepsilon_s B - aB^3 - bB^5$, in the long time limit when $B = dB/dt \rightarrow 0$, and under the conditions $a, b > 0$, with b negligible. At $\psi = \psi_t$, $a = 0$, and the b term must be included. The quantity $N - 1$ is proportional to the steady-state value of B^2 , so that well above ψ_t , $N - 1 \propto \varepsilon_s$, but for ψ_t , $N - 1 \propto \varepsilon_s^{1/2}$. As ψ_t is approached from above, the slope of the Nusselt curve diverges. Equation (1) implies that for $-\psi/\psi_t \gg 1$, a situation which hold for $\psi > 0$, excluding perhaps a narrow band near $\psi = 0$, $N_{1s} \approx 2L$ ($\lesssim 0.1$ for our experiments). Calculations using a five-mode model¹⁷ indicate, for $\psi > \psi_t$ (except very near ψ_t) and small L , that the Nusselt number will qualitatively change from the result of Eq. (1) as R is increased above R_{cs} . As in Fig. 1(b), when R exceeds

$$R_{cp} = [1 + \psi(1 + L^{-1})]R_{cs} = R_{cs}(\psi = 0), \quad (2)$$

the Nusselt number increases much more rapidly with R than Eq. (1) indicates, and to within corrections of $O(L)$, $N_1 = R_{cp} dN/dR$ approaches ψ -independent values. When $\psi = 0$, the Nusselt number will be that of a pure fluid.

A summary of the predictions discussed above includes (1) oscillatory convection at onset for $\psi \lesssim -4 \times 10^{-3}$; (2) a weak initial rise in N , starting at R_{cs} , for positive ψ not too close to zero; (3) an approach of the slope N_1 to a value which is ψ independent with corrections of $O(L)$, above R_{cp} and for the same ψ 's as (2); (4) tricritical behavior in the very narrow range $-6 \times 10^{-5} \lesssim \psi < 0$, where the slope of the Nusselt number varies from infinity to its pure-fluid value. Of these expectations, (2) and to a certain extent (3) are observed in these experiments. Given the small range over which tricritical behavior is predicted for L small, it is questionable whether (4) is experimentally detectable in liquid helium. In the following paragraphs we detail our observations.

We present in Figs. 1(a) and 2 the Nusselt number N as a function of R . Figs. 1(a) and 2 have $\Gamma = 8.56$ and a number of different values of T , the mean temperature of the layer. Values of ψ cannot be assigned with great accuracy.¹³ However, we estimate that for $\psi > 0$, $d\psi/dT \approx 3 \times 10^{-4} \text{ (mK)}^{-1}$, and we assume, as discussed below, that $\psi = 0$ for the temperature T_* with $T_* - T_\lambda = 86.9 \text{ mK}$.

We obtained these Nusselt data by increasing the heat flux Q in small steps starting below Q_c , the value of Q at the onset of convection. Typical step sizes are $0.015Q_c$. Between steps the system was allowed to equilibrate, a process which required up to 20 thermal diffusion times $t_v = d^2/\kappa$ in the vicinity of a transition. The values of R

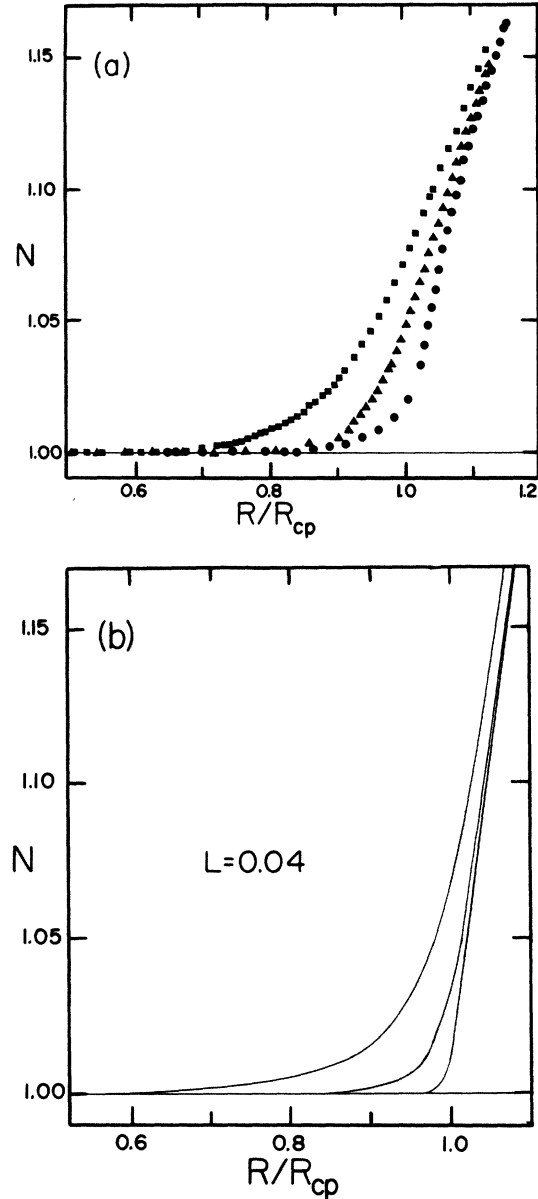


FIG. 1. (a) Values of the Nusselt number N vs R/R_{cp} for a ^3He mass concentration $c = 0.038$ and $\Gamma = 8.56$. Different symbols correspond to different values of T and, hence, different values of ψ . They are the following: squares, $T - T_\lambda = 187.0 \text{ mK}$; triangles, $T - T_\lambda = 109.6 \text{ mK}$; circles, $T - T_\lambda = 91.2 \text{ mK}$. The estimated values of ψ for these temperatures are 3.0×10^{-2} , 6.8×10^{-3} , and 1.3×10^{-3} , respectively. (b) Model calculations (see main text and Ref. 17) showing N vs R/R_{cp} for $L = 0.04$ and the estimated ψ 's of (a). Specifically, from left to right the curves correspond to $\psi = 3.0 \times 10^{-2}$, 6.8×10^{-3} , and 1.3×10^{-3} , respectively.

throughout this work have been presented in the form R/R_{cp} , where R_{cp} for each ψ has been chosen so that the experimental Nusselt numbers resemble model calculations,¹⁷ as in Fig. 1(b). For Fig. 1(b) we have used the five-mode model to calculate the Nusselt number for the same values of ψ as those which we estimate for the data of Fig. 1(a). However, unlike the five-mode model, the experimental results $N(R)$ become increasingly concave as

T approaches T_* from above. At T_* , the data can be fitted to the form $N - 1 = (\epsilon/f)^{0.5}$ with $f = 4.68$, as shown in Fig. 2(a). That $N(R)$ is found to be concave is somewhat surprising, since the model calculations indicate that concave behavior should occur over only an extremely narrow range of operating temperatures for the values of L typical of our experiments. Thus, if the system were to undergo a transition from pure-fluid-like behavior to tricritical behavior as ψ goes from 0 to -6×10^{-5} , $N(R)$ would be concave over a range of operating temperatures less than 0.2 mK wide. This conclusion is based on our estimate that near $\psi = 0$, $d\psi/dT \approx 3 \times 10^{-4} \text{ (mK)}^{-1}$.

If ψ is made more negative than the value ψ_* of ψ at T_* , as, for example, in Fig. 2(b), the first visible transition is a backward bifurcation. This transition, which corresponds to the lowest arrow in Fig. 2(b) is also signaled by long relaxation times. The hysteresis at the transition is quite small, about 0.1% of ΔT , and does not increase with decreasing ψ .

Time-dependent flow first occurs at the upper terminus of the Nusselt curves of Figs. 1(a) and 2. This time dependence is in many ways similar to what we have observed in pure ⁴He confined in cylindrical containers¹¹ and is associated with a secondary instability (skewed varicose instability in a pure fluid). It is striking that we do not observe oscillations at onset which are expected for values of $\psi \lesssim -L^2 \approx -2 \times 10^{-3}$. Indeed, for ψ as low as -0.2 , no oscillations were seen at the onset of convection. In this regard, we note that Rehberg and Ahlers¹⁰ have recently reported results on convection in a ³He-⁴He mixture confined in a rectangular layer of a porous medium which showed periodic flow and behavior consistent with a codimension-two bifurcation.⁶ The temperature resolution

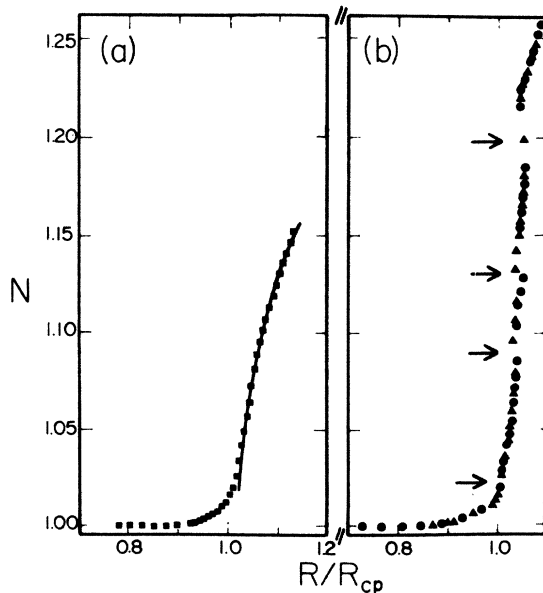


FIG. 2. Values of N vs R/R_{cp} for $c = 0.38$ and $\Gamma = 8.56$. (a) Data for T_* with $T_* - T_\lambda = 86.9$ mK; the solid curve satisfies $N - 1 = (\epsilon_s/4.86)^{0.5}$. (b) Data for a temperature less than T_* : $T - T_\lambda = 47.2$ mK ($\psi \approx -0.2$). The filled circles in (b) correspond to increasing heat flux and the filled triangles correspond to decreasing heat flux. The arrows indicate transition points.

in both the experiments of Rehberg and Ahlers and our own is comparable. If periodic flow existed with a similar amplitude in our experiments we would have observed it. Ahlers and Rehberg¹⁸ have made subsequent measurements on bulk ³He-⁴He mixtures confined in a rectangular geometry. They too find that there is no Hopf bifurcation in the vicinity of the expected polycritical value of ψ , although they do see oscillations at the onset of convection for $\psi < -0.015$. It is interesting that these experimenters see behavior for ψ near zero which resembles non-Boussinesq convection in a pure fluid.

For $\psi < \psi_*$, we see a number of secondary transitions above the onset of convection which are beyond the scope of present theory. Some of these are clearly hysteretic; in other cases the presence of hysteresis is not so strongly established. The transition marked by the second to lowest arrow in Fig. 2(b) first occurs at a value of ψ , which is just slightly less than ψ_* . The last transition before the onset of time-dependence when $\psi < \psi_*$ typically is hysteretic, is followed at higher N by a section of nearly infinite slope, and then a section of relatively smaller slope.

It is interesting to see if the critical Raleigh numbers which we obtain experimentally for $\psi > \psi_*$ are in agreement with relevant predictions. In Fig. 3 we compare experimental values of R_{cs} , defined by the start of the initial rise of $N(R)$, and experimental values of R_{cp} with predictions^{5,8} for R_{cs} which apply for rigid boundaries and a horizontally infinite layer. We also show experimental values of the critical Rayleigh number for $\psi < \psi_*$. For the purpose of comparing to theory, we assume that the value of ψ at T_* is zero. At T_* , we find an onset Rayleigh number of $1.4 \times 10^3 \pm 0.4 \times 10^3$, in acceptable agreement with the expected value 1708. We have then uniformly normalized our values of R_{cs} to yield 1708 at $T - T_\lambda = 86.9$ mK in order to remove most of the systematic uncertainty associated with the parameters β_1 , d , ν , and κ contained in R . A comparison of our data and calculations for R_{cs} at larger

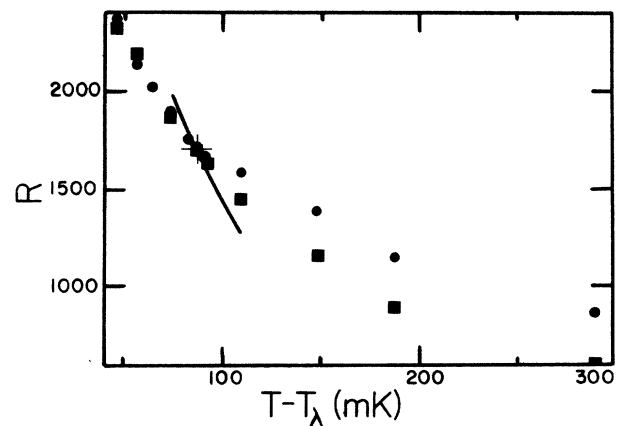


FIG. 3. Critical values of R as a function of $T - T_\lambda$. The temperature T_* with $T_* - T_\lambda = 86.9$ mK lies at the cross. For $T - T_\lambda$ less than this value, the onset to convection occurs as a discontinuous transition. Values of R_{cs} which are predicted for rigid boundaries are shown as a solid line, using the best estimate of ψ . Experimental values of R_{cp} (filled circles) and R_{cs} (filled squares) have been normalized by a common factor so that $R_{cp} = R_{cs} = 1708$ at $T - T_\lambda = 86.9$ mK.

values of ψ is difficult because for the small ψ 's involved, the uncertainties in ψ are *at least* 100%;¹³ experimental data for the parameters in ψ extend up to $T - T_\lambda = 100$ mK at best, and errors in ψ are amplified by factors of L^{-1} in the expressions for R_{cs} . With this caveat, we show as a solid line the calculated values of R_{cs} vs T based on our estimates of ψ ; the temperature $T - T_\lambda = 86.9$ mK is indicated by the cross. We find that the temperature variation of the experimental determinations of R_{cs} is in acceptable agreement with predictions. Results for R_{cp} shown in Fig. 3 are also interesting. The values we show in Fig. 3 were obtained by requiring qualitative agreement between the five-mode model and the data. Our results for R_{cp} tend to decrease with ψ , in contrast to model results, but we do not see this as a major problem in light of the limited nature of the model.

We have made additional measurements at other aspect ratios in order to test for the possibility of non-Boussinesq effects. That is, we wanted to see if variations of the fluid properties throughout the layer could affect the resulting flow. This is particularly important because typical experimental temperature differences across a layer may often be large enough that the accompanying variations in ψ may be comparable to $|\psi_{pc}|$ and/or $|\psi_t|$. This applies to both the present experiments and those of Refs. 10 and 18. It is possible to test experimentally for departures from the Boussinesq approximation by performing measurements on layers of different heights d . The value of ΔT at onset varies as d^{-3} , when all other parameters are unchanged. If d is decreased, any departure from the Boussinesq approximation will grow. In the present experiments we could vary d at fixed δ , hence changing Γ . We made additional measurements with $\Gamma = 5.51$ and $\Gamma = 10.16$, so that ΔT at onset varied by a factor of about 6.3. These measurements reproduced the same features found for $\Gamma = 8.56$, and non-Boussinesq effects were not detected.

Previous experiments by Lee, Lucas, and Tyler⁵ have been made on bulk ^3He - ^4He mixtures in cylindrical containers. These authors reported results for critical values of R , but they did not present results for the Nusselt number, and consequently they did not report any of the behavior which we observe.

To conclude, we note that these experiments have shown qualitative similarities to predictions, but also some differences. The data for $\psi > 0$ show the weak initial rise expected near the onset of convection and a qualitative resemblance to calculations. However, for $\psi = 0$, N is a concave function of R over a much broader range of ψ than in model calculations. We have not observed the predicted oscillations at the onset of convection for $\psi < 0$. Experiments¹⁸ made on a similar mixture contained in a rectangular geometry are significantly different from ours. This result is surprising because in pure ^4He flow the onset of convection, as manifested in heat-flow experiments, is not particularly sensitive to differences between cylindrical and rectangular geometry. Several theoretical and experimental issues must be confronted if this puzzle is to be solved. These issues include an understanding of the effect of variations of ψ throughout the layer, a knowledge of the patterns formed by the convection rolls with their relation to the sidewall geometry, better data for the fluid parameters, particularly ψ , and an understanding of the effect of nonslip boundaries on calculations.

We acknowledge several useful conversations with Professor G. Ahlers, Professor P. Hohenberg, Professor P. Kolodner, Professor C. Surko, and Professor R. Walden. This work has been supported by the National Science Foundation under Low-Temperature Physics Grant No. DMR-8314673. One of us (R.P.B) acknowledges support from the Alfred P. Sloan Foundation.

¹For a review see *Physica D* **7**, 1 (1983).

²For a recent review of Rayleigh-Benard convection with an emphasis on cryogenic experiments, see R. P. Behringer, *Rev. Mod. Phys.* **57**, 657 (1985).

³R. S. Schechter, M. G. Velarde, and J. K. Platten, in *Advances in Chemical Physics*, edited by I. Prigogine and S. A. Rice (Wiley, New York, 1974), Vol. 26, and references therein.

⁴R. W. Walden, P. Kolodner, A. Passner, and C. M. Surko, *Phys. Rev. Lett.* **55**, 496 (1985).

⁵G. W. T. Lee, P. Lucas, and A. Tyler, *J. Fluid Mech.* **135**, 235 (1983).

⁶H. Brand, P. C. Hohenberg, and V. Steinberg, *Phys. Rev. A* **30**, 2548 (1984).

⁷H. Brand and V. Steinberg, *Phys. Lett.* **93A**, 333 (1983).

⁸D. Gutkowicz-Krusin, M. A. Collins, and J. Ross, *Phys. Fluids* **22**, 1443 (1979); **22**, 1451 (1979).

⁹R. S. Schechter, I. Prigogine, and J. R. Hamm, *Phys. Fluids* **15**, 379 (1972).

¹⁰I. Rehberg and G. Ahlers, *Phys. Rev. Lett.* **54**, 500 (1985).

¹¹R. P. Behringer, H. Gao, and J. N. Shaumeyer, *Phys. Rev. Lett.* **50**, 1199 (1983); H. Gao and R. P. Behringer, *Phys. Rev. A* **30**, 2837 (1984); G. Metcalfe, T. Jung, H. Gao, and R. P. Behringer, *J. Fluid Mech.* (to be published).

¹²For a review of experimental parameters, see Ref. 5; R. P.

Behringer and H. Meyer, *J. Low Temp. Phys.* **46**, 407 (1982); D. Gestrich, R. Walsworth, and H. Meyer, *ibid.* **54**, 37 (1984).

¹³Experimental determinations of ψ are made by deducing ψ from measurements of β_1 and the quantity $\alpha = \beta_1(1 + \psi)$. Both α and β_1 have systematic uncertainties of several percent. In the vicinity of $\psi = 0$, these systematic errors in α and β_1 cause very large errors in ψ .

¹⁴P. H. Couillet and E. A. Spiegel, *SIAM J. Appl. Math.* **43**, 776 (1983); J. Guckenheimer, *SIAM J. Math. Anal.* **15**, 1 (1984).

¹⁵In Ref. 6 above, the authors have used slip boundary conditions for the tangential velocity at the horizontal boundaries and assumed that deviations from the uniform conductive concentration distribution vanish there. The conditions which apply to experiments are vanishing tangential velocity and vanishing impurity flux. The choice of boundary conditions for the normal velocity and the temperature in Ref. 6 corresponds to experimental conditions.

¹⁶See, for instance, L. A. Segel, *J. Fluid Mech.* **38**, 203 (1969); A. C. Newell and J. A. Whitehead, *ibid.* **38**, 279 (1969).

¹⁷G. Veronis, *J. Mar. Res.* **23**, 1 (1964).

¹⁸G. Ahlers and I. Rehberg, *Phys. Rev. Lett.* **56**, 1373 (1986); G. Ahlers (private communication).